JOURNAL OF MATERIALS SCIENCE 28 (1993) 4398–4404

Mechanical strength of ultra-fine Al–AlN composites produced by a combined method of plasma–alloy reaction, spray deposition and hot pressing

A. INOUE, K. NOSAKI*, B. G. KIM, T. YAMAGUCHI‡, T. MASUMOTO
Institute for Materials Research, Tohoku University, Sendai 980, Japan

Ultra-fine Al–AlN composites with high packing density were produced by the simple sequential process consisting of nitrogen plasma–alloy reaction, spray deposition and hot-pressing. The AlN content, V_f, was controlled in the range below about 40 vol % by changing the nitrogen partial pressure in the plasma–alloy reaction. The density of the Al–AlN composite with $V_f = 36\%$ after hot-pressing for 7.2 ks at 673 K was 2.96 Mg m^{-3} which is nearly the same as the theoretical density. The constituent phases were f c c aluminium and hexagonal AlN and their lattice parameters are nearly the same as those of pure aluminium and AlN phases. The grain size and interparticle spacing of the AlN particles were as small as about 90 and 50 nm, respectively. The Vickers hardness number, Young's modulus and compressive strength of the dense Al–AlN composite were 193, 112 GPa and 628 MPa, and the high hardness above 100 was maintained in the temperature range below 673 K. It was therefore concluded that the sequential process is a useful technique to produce ultra-fine metal–ceramic composites with high mechanical strengths.

1. Introduction

It has recently been reported [1–3] for rapidly solidified Al–Ln–Ni (Ln = lanthanide metal) alloys that the homogeneous dispersion of nanoscale f c c aluminium particles with a size of 3–7 nm into an amorphous matrix gives rise to an increase in tensile fracture strength by about 1.5 times as compared with that for the amorphous single phase with the same alloy composition. Thus, nanocrystalline materials exemplified for the nanoscale composite have attracted increasing interest because of the appearance of unique characteristics which cannot be obtained for conventional crystalline alloys. Most recently, we have carried out a series of studies on the synthesis of nanocrystalline materials by various techniques such as consolidation of ultra-fine powders prepared by chemical reduction in aqueous solutions [4, 5], low-temperature crystallization of an amorphous phase [6, 7] and spray deposition of ultra-fine powders prepared by a plasma-alloy reaction [8, 9], with the aim of searching for unique characteristics caused by the nanoscale structure control. It is very much expected that a composite material consisting of ultra-fine hexagonal AlN particles embedded in an f c c aluminium matrix with a grain size below 100 nm may be prepared by a combined method of plasma–alloy reaction, spray deposition and hot-pressing, and that it would exhibit significantly improved mechanical strengths. The present work examined the microstructure, density, hardness and compressive strength of the hot-pressed compacts in an Al–AlN system, to investigate the effect of ultra-fine structure control on the mechanical strengths.

2. Experimental procedure

The newly designed experimental apparatus used in the present study is illustrated in Fig. 1. The equipment consists of a reaction chamber between nitrogen plasma and molten alloy and a spray deposition chamber. A pre-melted pure aluminium ingot weighing about 10 g was placed on a water-cooled copper anode plate in the atmosphere-controlled reaction chamber and remelted using an arc of a constant current at 200 A for a time of 180 s in different gas mixture ratios, P_n, of nitrogen to argon ranging from 0.1–1.0. The total pressure of nitrogen and argon was changed in the range 48–93 kPa. The difference in gas pressure between the two chambers was controlled in the range 48–93 kPa by adjusting both gas pressure at the inlet gate and the degree of evacuation at the outlet gate. The arc was generated by a tungsten inert gas (TIG) welding machine. The distance between the

Permanent address: Honda Research and Development Co. Ltd, Wako 351-01, Japan.

‡*Permanent address*: Research and Development Division, Yoshida Kogyo K. K., Kurobe 938, Japan.

0022–2461

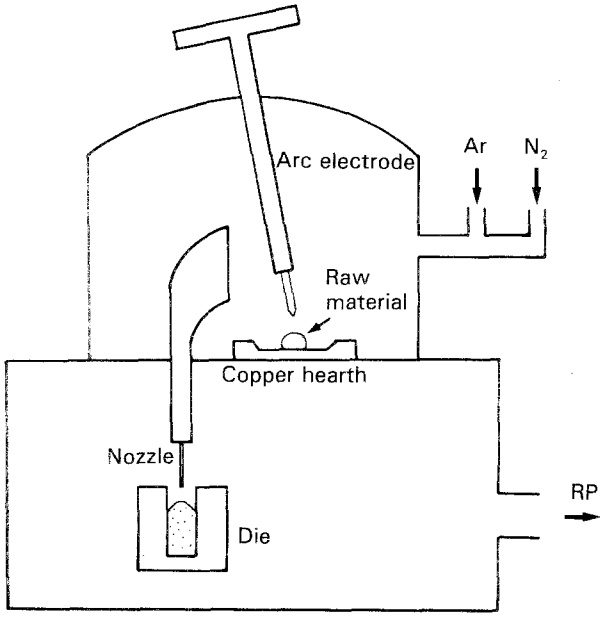

Figure 1 Schematic illustration of the equipment used for the formation of an Al–AlN composite with nanoscale particle sizes by a combined technique of nitrogen plasma–molten aluminium reaction and spray deposition.

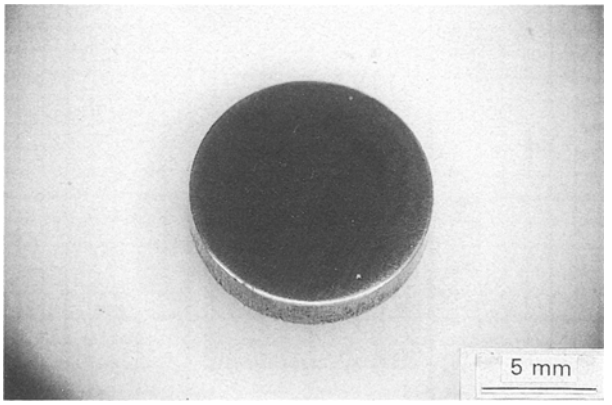

Figure 2 External appearance of a cold-pressed Al–AlN compact with $V_f = 36\%$ produced by a combined technique of nitrogen plasma–aluminium reaction, spray deposition and cold pressing.

tungsten cathode and the anode sample was maintained in the range 5–10 mm. The area of the suction gate was 2600 mm^2 and the diameter of the deposition nozzle was fixed at 2.0 mm. The suction gate was set at a position where the distance between the centre of the gate and the centre of the anode copper plate was about 110 mm. The sucked particles were deposited directly into the hot-pressed die with an inner diameter of 10 mm and the spray time was changed in the range 180–900 s. The spray-deposited particles were pressed for 180 s under a uniaxial compressive stress of 1000 MPa at room temperature. The resulting cold-pressed compact had a disc shape with different heights ranging from about 2–10 mm. Subsequently, the cold-pressed compact was subjected either to sintering for 3.6 ks in the temperature range 473–673 K, or to hot-pressing under a constant applied stress of 245 MPa for different periods of 1.8–10.8 ks at temperatures between 473 and 673 K. Nitrogen and oxygen contents were measured by chemical analyses.

The structure and outer morphology of the cold- and hot-pressed compacts were examined by X-ray diffractometry and transmission electron and optical microscopy (TEM and OM) techniques. The TEM thin foils were prepared by ion milling. The structure and morphology of the spray-deposited particles themselves were also examined in a short-time (3 s) deposited state by TEM. The density of the pressed compacts was measured by the Archimedian method using toluene. The hardness and compressive strength were measured by a Vickers hardness tester with a load of 500 g in the temperature range of room temperature to 873 K and an Instron-type testing machine at a strain rate of $8.3 \times 10^{-6}\ s^{-1}$ and room temperature, respectively.

3. Results and discussion

Fig. 2 shows an optical micrograph revealing the surface appearance of a cold-pressed compact of the particles produced by the nitrogen plasma–molten alloy reaction under the conditions of $P_n = 1.0$ and a total pressure of 93 kPa. A disc sample with a fixed dimension (10 mm × 2 mm) and smooth surface was formed. The X-ray diffraction pattern taken from the cold-pressed compact consists of two phases of fcc aluminium and hexagonal AlN, as indexed in Fig. 3, indicating that the combined synthesis process can produce a bulky composite consisting of aluminium and AlN phases. The lattice parameter evaluated from the X-ray diffraction peaks is 0.4052 nm for aluminium and $a = 0.3111$ nm and $c = 0.4982$ nm for AlN, in agreement with those [10] for pure aluminium and stoichiometric AlN phases. No appreciable peak of any oxide is seen in the diffraction pattern. The chemical analyses of nitrogen and oxygen contents were made for the cold-pressed compacts of particles produced under different nitrogen partial pressures. Table I summarizes the chemically analysed nitrogen and oxygen contents, the volume fraction of AlN calculated from the chemically analysed nitrogen content and the measured density for the cold-pressed compacts. With increasing nitrogen pressure from 24–93 kPa, the nitrogen content increased continuously from 1.16–14.7 wt %, accompanying the increase in density resulting from the increase in the

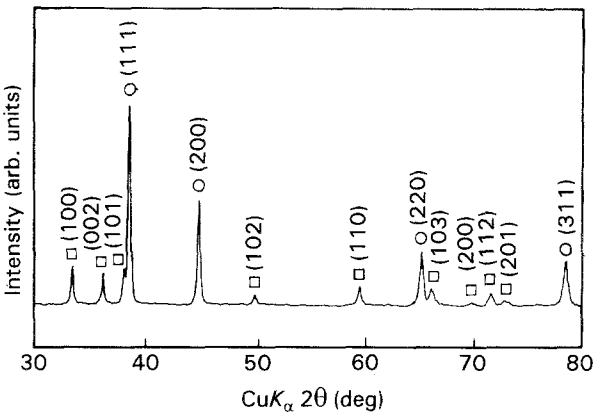

Figure 3 X-ray diffraction pattern of a cold-pressed Al–AlN compact with $V_f = 36\%$ produced by the combined technique. (○) Al, (□) AlN.

TABLE I Nitrogen and oxygen contents obtained by chemical analyses, volume fraction of AlN calculated from the nitrogen contents and measured density for cold-pressed compacts of the AlN and aluminium particles produced in different nitrogen partial pressures

N_2 partial pressure (kPa)	Nitrogen content (wt %)	AlN, V_f (%)	Density (Mg m^{-3})	Oxygen content (wt %)
24	1.16	2.8	2.74	1.25
48	8.37	21.9	2.88	1.76
80	12.5	32.8	2.93	2.07
93	14.7	36.5	2.95	2.04

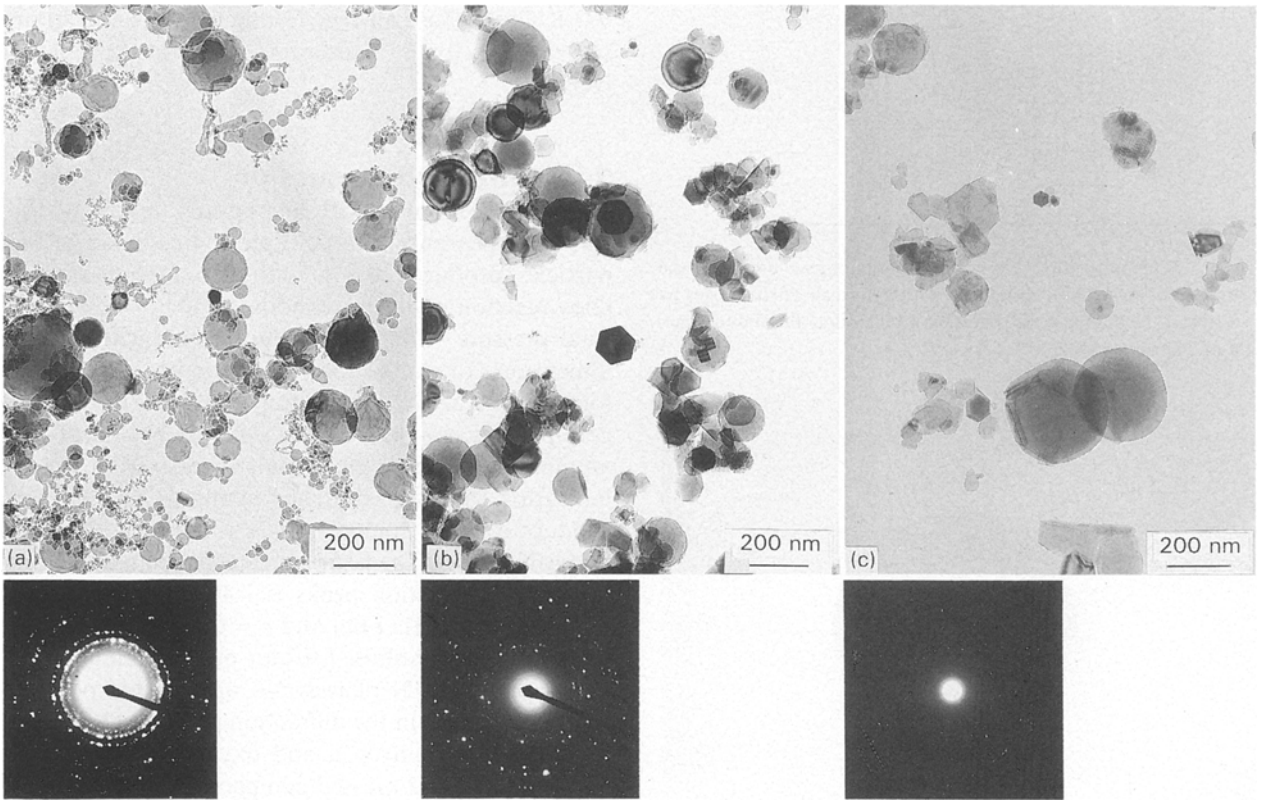

Figure 4 Bright-field electron micrographs and selected-area diffraction patterns of the deposited particles produced by the nitrogen plasma–aluminium reaction and spray deposition technique. The spray time is as short as 3 s. (a) $P_n = 0.5$, total pressure = 48 kPa; (b) $P_n = 1.0$, total pressure = 48 kPa; (c) $P_n = 1.0$, total pressure = 80 kPa.

dissolution amount of nitrogen. Furthermore, it was noticed that the volume fraction of AlN phase could be controlled in the range below 40%, by using the present combined synthesis method. On the other hand, the oxygen content lay in the range of 1.25 and 2.07 wt % and was independent of nitrogen pressure. The mixing of elemental oxygen may be due to the exposure to air before chemical analysis, as well as the residual existence of a trace amount of oxygen in the mixed nitrogen and argon gases used for the plasma–alloy reaction.

Here, it is important to clarify the microstructure and morphology of the particles themselves produced by the nitrogen plasma–alloy reaction method under different nitrogen partial pressures. Fig. 4 shows the changes in bright-field electron micrographs and selected-area electron diffraction patterns of the mixed aluminium and AlN particles deposited under different conditions of P_n and total pressure. The morphology of the particles is mainly spherical at $P_n = 0.5$ and a total pressure of 48 kPa and the mean diameter is as small as 50 nm. The electron diffraction rings taken from these spherical powders are identified as fcc structure with strong reflection rings and an hcp structure with weak reflection rings, indicating that the spherical powder is composed mainly of an fcc phase. With increasing mixing ratio and total nitrogen pressure, one can see clearly the ultra-fine particles with a hexagonal shape, in addition to the spherical aluminium powders, together with the superposition of the diffraction rings of a hexagonal AlN phase on those of the fcc aluminium phase. Furthermore, the amount of hexagonal AlN powder tends to increase with increasing nitrogen gas pressure.

Fig. 5 shows an optical micrograph revealing the etched surface structure of the cold-pressed Al–AlN compact containing AlN phase of 36% volume fraction. No distinct void can be observed, indicating that the cold-pressing to the ultra-fine powder causes the formation of a highly dense bulk. Furthermore, two kinds of contrast can be seen, though the contrast pattern is very fine. Because the bright and dark

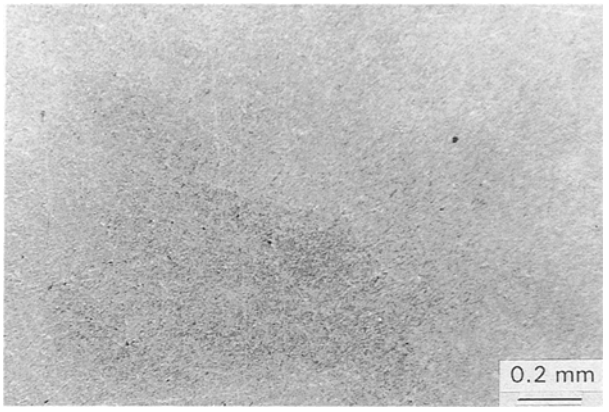

Figure 5 Optical micrograph revealing the structure of a cold-pressed Al–AlN compact with $V_f = 36\%$ produced by the combined technique.

contrasts correspond to AlN and aluminium phases, respectively, the bulk appears to be composed of two homogeneously mixed phases. Fig. 6 shows the changes in the calculated and measured densities and Vickers hardness as a function of the volume fraction of AlN phase, V_f, for the cold-pressed compacts. With increasing V_f from 2.8% to 36.5%, the measured density and hardness increase significantly from 2.73 Mg m^{-3} to 2.90 Mg m^{-3} and 96 to 164, respectively. The density is considerably lower for the measured value than for the calculated value because of the residual existence of voids.

The effect of sintering and hot-pressing on the density and hardness was examined for the cold-pressed Al–AlN compact with $V_f = 36\%$ with the aim of obtaining a composite material with high density and high hardness. Fig. 7 shows the changes in the density and Vickers hardness of the Al–AlN compact with sintering temperature. By sintering for 3.6 ks at 673 K, the density and hardness increase slightly to 2.92 Mg m^{-3} and 174, respectively. However, the increasing rate is as small as 0.7% for density and 6.1% for hardness, resulting in a density which is considerably smaller than the calculated value. This result suggests that the production of a dense bulk with true density only by sintering is rather difficult, even for the composite consisting of ultra-fine particles. Therefore, subsequent study was focused on the hot-pressed compacts. Fig. 8 shows the density and Vickers hardness as a function of hot-pressing temperature for 1.8 ks under an applied stress of 245 MPa for the Al–AlN composite with $V_f = 36\%$. The density and hardness increase with increasing pressing temperature and reach 2.93 Mg m^{-3} and 184, respectively, at 673 K. Although the density and hardness are larger than those of the sintered material, the density is about 99% of the calculated value.

In order to increase further the density of the pressed compact, the changes in the density and hardness as a function of pressing time at 673 K under the same pressure of 245 MPa were examined for the Al–AlN composite with $V_f = 36\%$. As shown in Fig. 9, the density and hardness increase parabolically with increasing pressing time and show nearly constant values of 2.96 Mg m^{-3} and 193, respectively, after

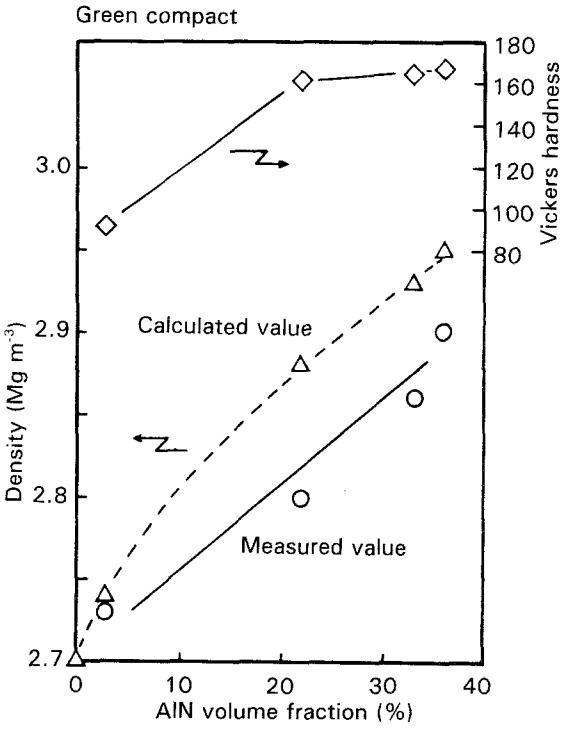

Figure 6 Density and Vickers hardness as a function of volume fraction of AlN phase, V_f, for a cold-pressed Al–AlN compact. The calculated density represents the value evaluated from the chemically analysed nitrogen content.

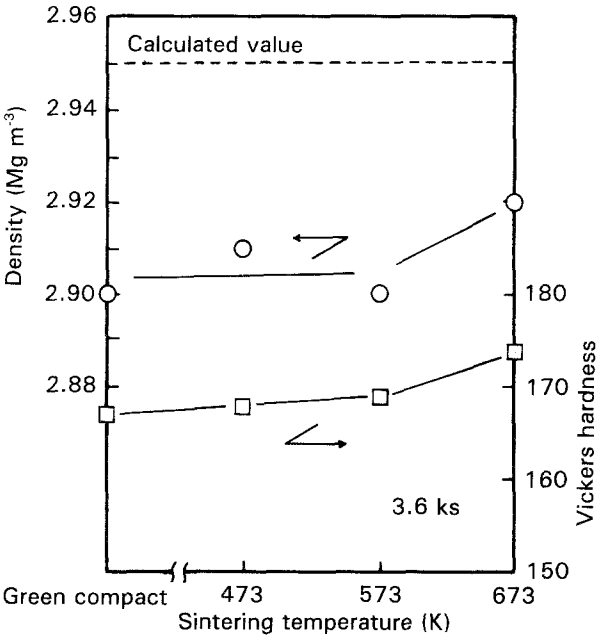

Figure 7 Density and Vickers hardness as a function of sintering temperature for a cold-pressed Al–AlN compact with $V_f = 36\%$.

7.2 ks. Although the reason for the density exceeding the calculated value remains unclear, it is said that the hot-pressing treatment for 7.2 ks at 673 K can produce a highly dense composite consisting of aluminium and AlN phases. The saturated hardness of 193 for the Al–AlN composite produced by hot pressing for 7.2 ks at 673 K is about 1.4 times as high as that ($H_V \simeq 140$) [11] of a high-strength type 7075-T6 alloy. In order to confirm the homogeneous dispersion of ultra-fine AlN particles embedded in fcc aluminium matrix and to

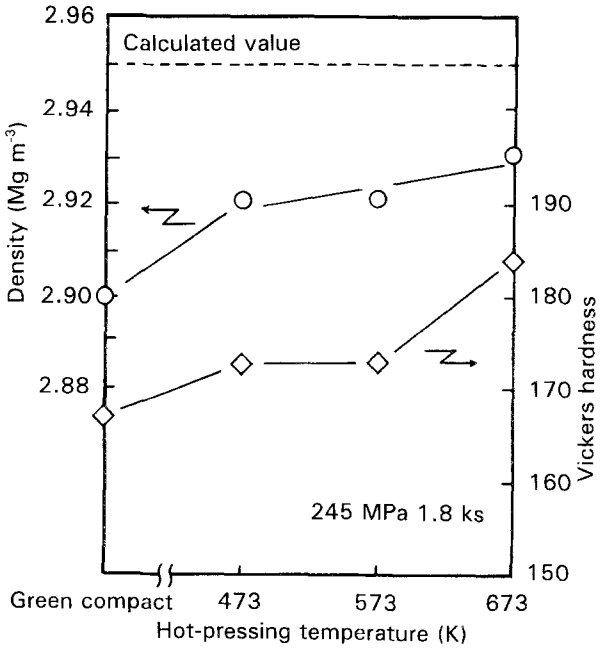

Figure 8 Density and Vickers hardness as a function of pressing temperature for a cold-pressed Al–AlN compact with $V_f = 36\%$.

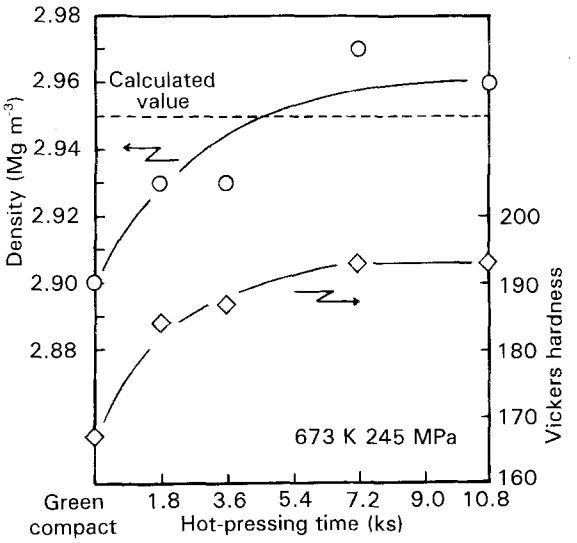

Figure 9 Density and Vickers hardness as a function of pressing time at 673 K for a cold-pressed Al–AlN compact with $V_f = 36\%$.

clarify the interfacial structure between aluminium and AlN phases, TEM observation was made for the Al–AlN composite with $V_f = 36\%$ produced by hot-pressing for 7.2 ks at 673 K. As exemplified in Fig. 10, AlN particles with an average size of about 90 nm disperse homogeneously with an interparticle spacing of about 50 nm in the f c c aluminium matrix. As the average particle size of AlN and aluminium is about 50 nm in the as-prepared state, the subsequent hot-pressing causes an increase of the grain size of AlN and aluminium through coalescence and growth mechanism even at a relatively low temperature of 673 K. Because the pressing temperature is about one-quarter of the decomposition temperature (2789 K) [12] of AlN, it is concluded that the ultra-fine AlN and aluminium particles have a good compactability

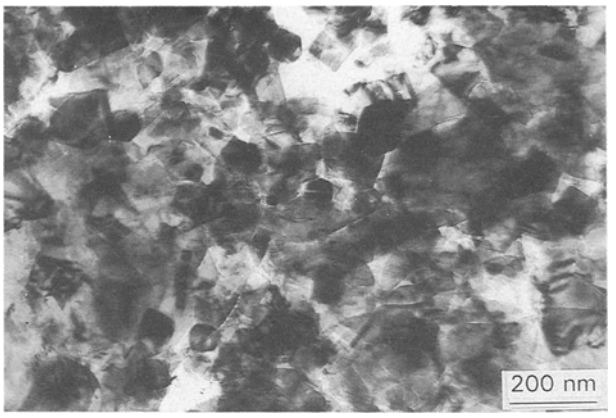

Figure 10 Transmission electron micrograph revealing the microstructure of an Al–AlN composite with $V_f = 36\%$ produced by hot-pressing for 7.2 ks at 673 K after cold pressing.

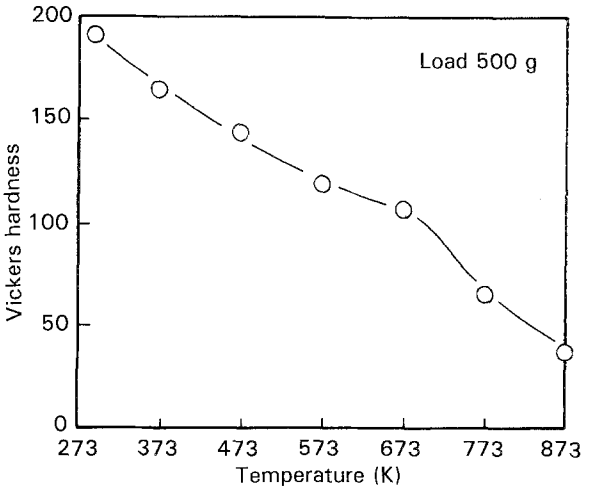

Figure 11 Vickers hardness as a function of testing temperature for an Al–AlN composite with $V_f = 36\%$ produced by hot-pressing for 7.2 ks at 673 K after cold pressing.

through high capability of coalescence and growth between the particles.

The homogeneous dispersion of ultra-fine AlN particles is expected to cause the suppression of the decrease in hardness at elevated temperatures on the basis of the mechanisms of dispersion hardening due to the AlN phase, and refinement hardening resulting from the suppression of grain growth due to the existence of AlN phase. Fig. 11 shows the Vickers hardness as a function of testing temperature for the Al–AlN composite with $V_f = 36\%$. The high hardness number above 100 is maintained in the wide temperature range up to 673 K. It should be noted that the high hardness number ($\simeq 100$) at 673 K is about 15 times as high as that ($\simeq 7$) [13] for a commercial 2017-T6 alloy with high heat-resistant strength. It is therefore concluded that the present metal–ceramic composite has an extremely high resistance against high-temperature deformation.

In addition to the Vickers hardness, compressive strength was measured for the Al–AlN composites with $V_f = 36\%$. The tested sample was a cylinder with a diameter of 10 mm and a height of 10 mm. As

summarized in Fig. 12, the compressive strength increases in the order of cold-pressed < sintered (673 K, 3.6 ks) < hot-pressed (673 K, 7.2 ks) and the highest value reaches 628 MPa which is higher than the fracture strength (516 MPa) [14] for the 2024-T6 alloy containing SiC powder of $V_f = 20\%$ produced by a hot-forging treatment of powders. The Young's modulus, E, evaluated from the compressive stress–strain curves is 112 GPa for the Al–AlN composite produced by hot pressing for 7.2 ks at 673 K. The value of E is about 1.6 times as high as that (79.6 GPa) [15] for the conventional high-strength type aluminium-based alloys, indicating that the homogeneous dispersion of the AlN particle into the aluminium matrix is effective for the increase in stiffness. Fig. 13 shows a scanning electron micrograph revealing the fracture surface appearance of the Al–AlN composite with $V_f = 36\%$ produced by hot-pressing for 7.2 ks at 673 K. It is again confirmed that the composite contains homogeneously ultra-fine AlN particles with an average particle size of about 100 nm. The particle size remains almost constant after hot-pressing at 673 K. However, no distinct contrast revealing the existence of isolated ultra-fine aluminium particles is seen for the hot-pressed composite, indicating the progress of coalescence among the aluminium particles and between the aluminium and AlN particles.

Here, we investigate the measured E value on the basis of a mixing rule which has been proposed [16] to be applied for the mixed-structure materials containing dispersed spherical particles. The mixing rule for E has been presented as

$$\ln E_c = V_f \ln E_{AlN} + (1 - V_f) \ln E_{Al} \quad (1)$$

where E_c, E_{Al} and E_{Aln} are the Young's moduli of the composite material, pure aluminium and stoichiometric AlN, respectively. The E_{Al} and E_{AlN} values used in the present evaluation are 70.6 GPa [15] and 294 GPa [17], respectively. The calculated E value for the mixed material with $V_f = 36\%$ is 118 GPa, which is nearly the same as the measured E value (112 GPa). The rather good agreement indicates that the present sequential process facilitates the production of highly dense composite bulk materials with ultra-fine grain sizes. In addition, when the mixing rule is assumed to be applied for H_v, the calculated H_v value for the composite material is 85, which is much smaller than the measured value (193). Here, the H_v values of aluminium and AlN phases used in the calculation are 20 [15] and 1100 [18], respectively. The considerably larger H_v value of the present Al–AlN composite may be due to a refinement effect of the composite structure.

4. Conclusion

Production of ultra-fine Al–AlN composites by a combined technique consisting of nitrogen plasma–alloy reaction, spray deposition and hot-pressing and clarification of microstructure and mechanical properties were carried out with the aim of investigating the effect of ultra-fine structure on the mechanical properties. By controlling nitrogen partial pressure in the range

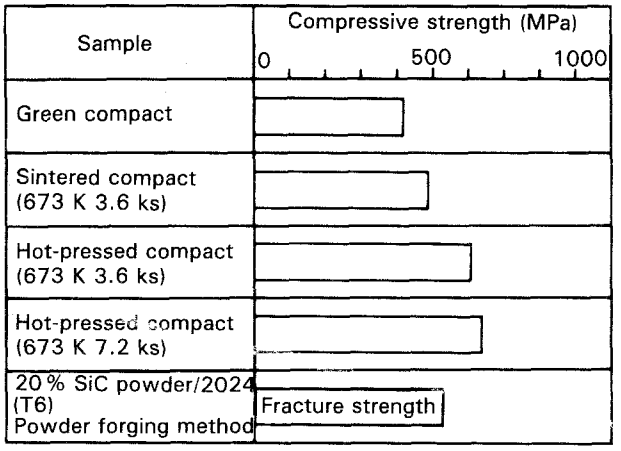

Figure 12 Compressive fracture strength of Al–AlN composites produced under different preparation conditions. The data [14] of a commercialized 2024(T6)–20% SiC composite produced by hot-forging are also shown for comparison.

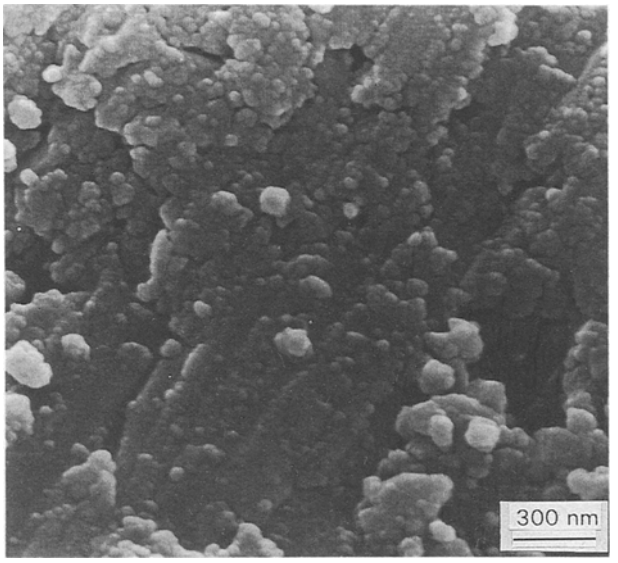

Figure 13 Scanning electron micrograph revealing the fracture surface appearance of an Al–AlN composite with $V_f = 36\%$ produced by hot-pressing for 7.2 ks at 673 K after cold pressing.

24–93 kPa, the nitrogen content in the resulting spray-deposited bulk was changed in the range 1.16–14.7 wt % corresponding to the formation of AlN ranging from 2.8%–36.5% volume fraction. The cold-pressed compact is composed of ultra-fine aluminium and AlN particles with a size of 50–150 nm. Hot-pressing for 7.2 ks at 673 K produces Al–AlN composites with a true density and grain size, and the interparticle spacing of the AlN particles retains the ultra-fine scale of about 90 and 50 nm, respectively. The hardness, Young's modulus and compressive strength of the hot-pressed Al–AlN composite containing AlN of 36% volume fraction are 193, 112 GPa and 628 MPa at room temperature, being comparable to those for an aluminium-based alloy (2024-T6) containing 20% volume fraction of SiC produced by hot forging. The hardness retains a very high level of about 100 even at 673 K because of the dispersion hardening of the ultra-fine AlN particles. Thus the simple sequential process of plasma–alloy reaction, spray deposition

and hot-pressing appears to be useful for the production of ultra-fine metal–ceramic composites exhibiting good mechanical strength. The production and characterization of similar composite materials consisting of metal–metal or ceramic–ceramic phases are in progress.

References

1. Y. H. KIM, A. INOUE and T. MASUMOTO, *Mater. Trans. JIM* **31** (1990) 747.
2. *Idem, ibid.* **32** (1991) 331.
3. *Idem, ibid.* **32** (1991) 599.
4. A. INOUE, J. SAIDA and T. MASUMOTO, *Met. Trans.* **19A** (1988) 2315.
5. J. SAIDA, A. INOUE and T. MASUMOTO, *Mater. Sci. Eng.* **A133** (1991) 771.
6. K. SUZUKI, N. KATAOKA, A. INOUE, A. MAKINO and T. MASUMOTO, *Mater. Trans. JIM* **31** (1990) 743.
7. K. SUZUKI, A. MAKINO, N. KATAOKA, A. INOUE and T. MASUMOTO, *ibid.* **32** (1991) 93.
8. A. INOUE, K. NOSAKI, B. G. KIM, T. YAMAGUCHI and T. MASUMOTO, *J. Mater. Sci. Lett.*, **11** (1992) 865.
9. *Idem, J. Appl. Phys.*, **71** (1992) 4025.
10. W. B. PEARSON, "Lattice Spacings and Structures of Metals and Alloys" (Pergamon Press, London, 1958) pp. 124, 980.
11. "Metals Databook", edited by Japan Institute of Metals (Maruzen, Tokyo, 1983) p. 176.
12. P. O. SCHIRSEL and W. S. WILLIAMS, *Bull. Am. Phys. Soc. II* **4** (1959) 139.
13. E. EVANGELISTA, A. FORCELLESE, F. GABRIELLI and P. MENGUCCI, in "Hot Deformation of Aluminum Alloys", edited by T. G. Langdon, H. D. Merchant, J. G. Morris and M. A. Zaidi (Minerals, Metals and Materials Society, Warrendale, PA 1991) p. 121.
14. S. J. HARRIS, in "Aluminum Alloys-Contemporary Research and Applications", edited by A. K. Vasudevan and R. D. Hoherty (Academic Press, Boston, MA, 1989) p. 255.
15. C. J. SMITHELLS, "Metals Reference Book", 5th Edn, (Butterworth, London, 1976) pp. 975, 1083.
16. Y. KAGAWA and H. HATTA, "Tailoring Ceramic Composites" (Agne, Tokyo, 1990) p. 96.
17. T. FUNAHASHI and K. ISOMURA, *Bull. Ceram. Soc. Jpn.* **26** (1991) 750.
18. Y. IMAI and S. KARASHIMA (eds), "Handbook of Heat-Resistant Materials" (Asakura Tokyo, 1965) p. 757.

Received 9 March 1992
and accepted 15 January 1993